Transactions on Environment, Energy and Earth Sciences
ISSN: 2960-1924, eISSN: 2960-2300 | Volume 5
EMCEME 2025

Electrochemical Water Oxidation for Hydrogen Peroxide Generation and Its Applications in Environment Fields

Jian Cai *

Acabrige College, Shanghai 200137, China

* Corresponding Author Email: 1931185679@qq.com

Abstract. Hydrogen peroxide (H_2O_2) is widely used in the field of biochemical disinfection due to its oxidizing property and environmental friendliness. Its demand is also increasing year by year in industries such as textiles, papermaking, and water treatment. The anthraquinone method is currently the main industrial method for producing H_2O_2, but this method involves multiple steps, and H_2O_2 separation and purification is difficult. The direct synthesis method also has problems such as high energy consumption and low safety. Instead, electrocatalytic water oxidation reaction (WOR) is a convenient, economical and environmentally friendly way, with advantages such as simple reaction conditions, clean production and safe reaction process. This review summarized the reaction mechanism, performance characterization, various electrocatalysts and modification methods, practical applications, summary and outlook for WORs for H_2O_2 production.

Keywords: Electrochemical Water Oxidation; H_2O_2 Generation; Modification strategy; Environmental applications.

1. Introduction

In recent years, hydrogen peroxide (H_2O_2), as a green and highly efficient oxidant, has been applied in various fields, such as the bleaching of paper and textiles, the synthesis of fine chemicals, wastewater treatment, mining and metal processing, semiconductor cleaning, sterilization and disinfection, and waste gas treatment, etc. [1, 2]. The demand for H_2O_2 in our country is extremely high. By the end of 2018, the domestic production capacity of H_2O_2 had reached 3.5 million tons per year, accounting for half of the global production capacity.

At present, the large-scale production of H_2O_2 above 95% is mainly achieved through the indirect anthraquinone (AQ) synthesis method [3]. AQ process mainly consists of four steps: hydrogenation of alkyl AQ, oxidation of hydrogenated anthraquinone, separation and purification of H_2O_2. Although AQ method is suitable for large-scale production, the operation process is complex, energy consumption is high, and the organic compounds formed in the products greatly increase the difficulty of H_2O_2 separation and purification. Moreover, a large amount of waste organic pollutants (trioctyl phosphate, aromatic compounds, and tert-butylurea) are discharged during the reaction, which is not conducive to the sustainable development of energy. In addition, during the entire process of transportation and storage from centralized factories to users, unstable H_2O_2 also poses safety risks. Thus, more safety methods are needed.

The direct synthesis method offers another option. In this method, the equation that occurs is: $H_2 + O_2 \rightarrow H_2O_2$. The mixed gas of O_2 and H_2 along with water is placed in a sealed container with a certain pressure. And H_2O_2 is produced using the precious metal Pd as a catalyst, where Pd can fix hydrogen. This direct synthesis method has solved the problems caused by the AQ method in some aspects, but this reaction requires the long-term exposure and mixing of H_2 and O_2, which is highly prone to explosion and has a high risk. Moreover, the use of precious metals increases the cost. Therefore, it is necessary to explore safer, more efficient and greener synthetic methods.

Electrocatalytic production of H_2O_2 can be easily realized, using electricity as the energy source and water as the raw material [4]. This method has the advantages of high efficiency and environmental friendliness, which has received increasing attention. Based on the redox properties, electrocatalytic

H_2O_2 production can be divided into two-electron oxygen reduction and water oxidation reactions (2e$^-$ ORR, WOR). Since 2e$^-$ WOR can produce H_2O_2 without relying on O_2, more and more researchers are focusing on WOR. This review will review the reaction mechanism, performance characterization, various electrocatalysts and modification methods, practical applications, summary and outlook for 2e$^-$ WORs.

2. Fundamental Basics of H_2O_2 Synthesis

2.1. Thermodynamics of H_2O_2 Synthesis

The device of the electrocatalytic electrolytic cell is divided into two parts - the anode and the cathode. The components include: the working electrode, the reference electrode, the counter electrode, and the electrolyte, etc. In principle, the water decomposition reaction primarily generates hydrogen gas (H_2) and oxygen gas (O_2) as the final products. During the electrocatalytic water decomposition process, the cathode undergoes a reduction reaction to produce hydrogen gas, while the anode undergoes WOR reaction. The electrocatalytic water oxidation reaction mainly includes (Eq 1-3, Figure 1): the one-electron process generates •OH; the two-electron process generates H_2O_2; and the four-electron process generates O_2. Among these three reactions, the oxygen evolution reaction is the most likely to occur (1.23 V vs. RHE). However, for the target product H_2O_2, the required theoretical potential is 1.76 V vs. RHE, which makes the thermodynamic generation of H_2O_2 more difficult. The one-electron reaction requires a theoretical potential of 2.73 V vs. RHE, meaning that generating •OH is the most difficult.

$$H_2O \rightarrow OH + e^- + H^+, E^\circ = 2.73 \text{ V vs. RHE} \tag{1}$$

$$2H_2O \rightarrow H_2O_2 + 2e^- + 2H^+, E^\circ = 1.76 \text{ V vs. RHE} \tag{2}$$

$$2H_2O \rightarrow O_2 + 4e^- + 4H^+, E^\circ = 1.23 \text{ V vs. RHE} \tag{3}$$

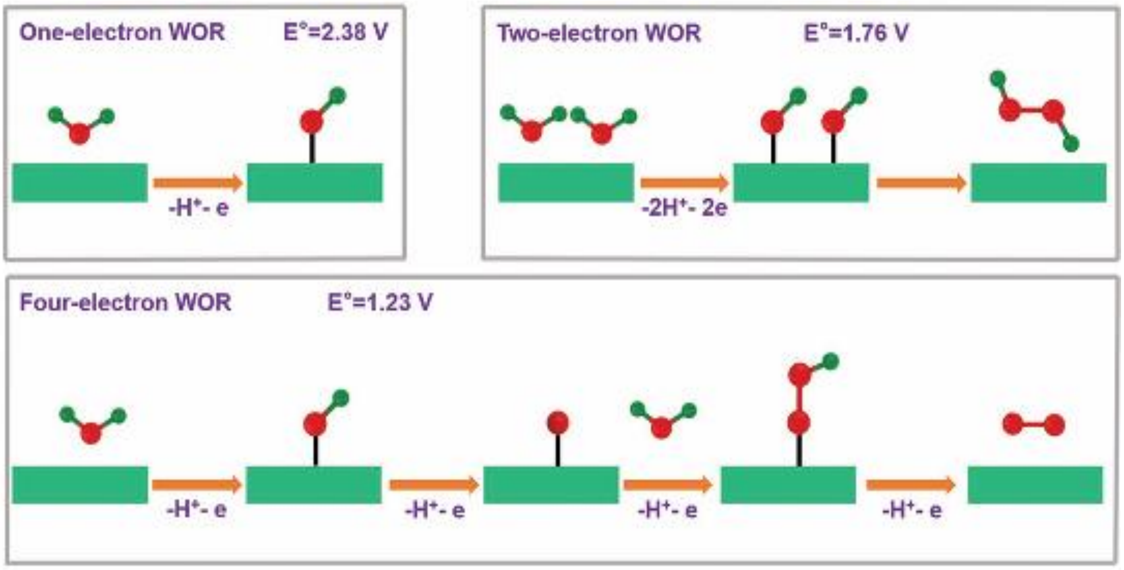

Figure 1. Three different reaction pathways for WORs.

2.2. Theoretical Calculations

The researchers used DFT calculations to explore the mechanism of the WORs. As shown in Figure 1, if the adsorption of OH* is weak, the 1e$^-$ reaction occurs; if it is strong, the 2 or 4e$^-$ reaction takes place. If the adsorption of O* is weak, a 2e$^-$ reaction occurs; if it is strong, a 4e$^-$ reaction occurs. Furthermore, the researchers obtained Figure 2 through DFT calculations. Based on the relationship between $\triangle G_{OH*}$ and $\triangle G_{O*}$ in (left), it can be seen that if $\triangle G_{OH*}$ is greater than 2.4 eV, the $1e^-$ reaction is more likely to occur; if $\triangle G_{OH*}$ is less than 2.4 eV while $\triangle G_{O*}$ is greater than 3.5 eV, the $2e^-$ reaction is more likely to occur; if $\triangle G_{OH*}$ is less than 2.4 eV while $\triangle G_{O*}$ is less than 3.5 eV, the $4e^-$ reaction is more likely to occur. Combining the relationship between $\triangle G_{OH*}$ and $\triangle G_{O*}$ ($\triangle G_{O*} = 2\triangle G_{OH*} + 0.28$), for water oxidation catalysts, $\triangle G_{OH*}$ needs to be less than 2.4 eV and greater than 1.6 eV in order to facilitate the production of the target substance H_2O_2.

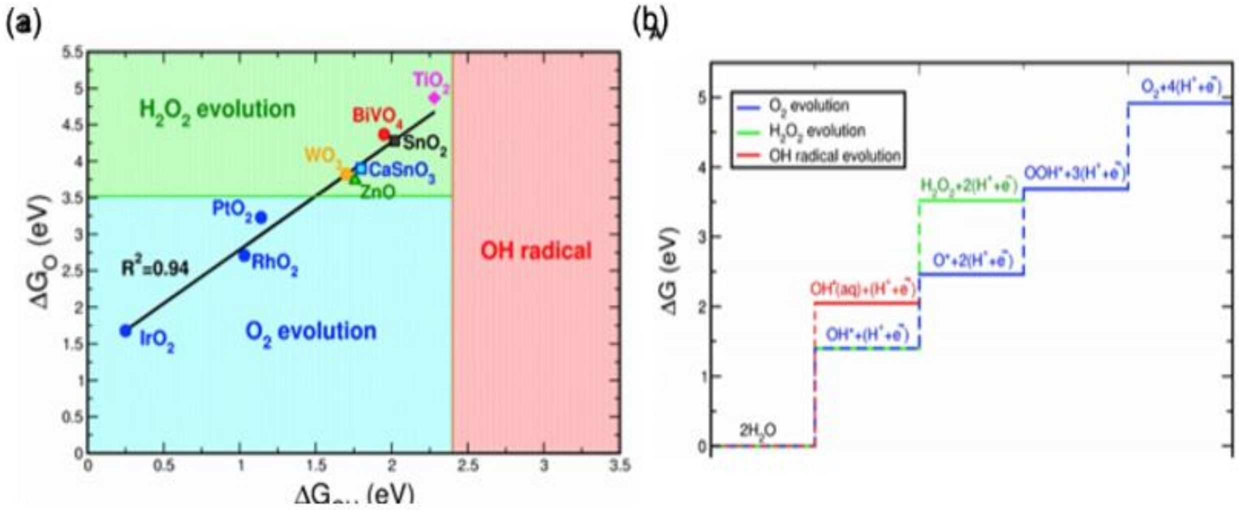

Figure 2. Selectivity and activity maps about three WORs based on thermodynamic.

3. Characterization of H2O2 Production Performance

3.1. Evaluation Parameters

The performance of electrocatalytic reactions is evaluated through three parameters: activity, selectivity and stability.

H_2O_2 activity is mainly obtained through linear sweep voltammetry (LSV) or cyclic voltammetry (CV) tests. For both materials, the larger the current signal value of LSV or CV, the stronger the activity. For overpotential, the smaller the η at 10 mA·cm^{-2}, the stronger the activity. Stability is tested through chronopotentiometry (CP) and repeated cycles.

H_2O_2 selectivity is determined by Faradaic efficiency (FE). The formula for calculating FE is:

$$\begin{aligned} FE &= \frac{Amount\ of\ generated\ H2O2}{Theoretically\ generated\ H2O2} \times 100\% \\ &= \frac{M_{H_2O_2}}{\frac{\int_0^t I(t)dt}{nF}} \times 100\% \end{aligned} \tag{3}$$

Among them, M represents the amount of moles that produce H_2O_2; I represent the current signal within the t range; n represents the number of electron transfers (n = 2), and F represents the Faraday constant (96485 C·moL^{-1}).

3.2. Quantitative Method for H_2O_2

The concentration measurement of H_2O_2 usually involves the use of H_2O_2 strips, titration, and measurements conducted with a UV-vis spectrophotometer. For the H_2O_2 strip, the concentration of H_2O_2 is determined by the color change of the test paper. The basic principle of titration method is the redox reaction between H_2O_2 and $KMnO_4$. The endpoint of the titration is when the solution changes from colorless to a light pink color, and the color does not change within 30 seconds. UV-

Vis is calculated based on the absorbance at a specific wavelength. The characteristic wavelength in iodometry is 551 nm.

The common concentration of H_2O_2 is in units of mol L^{-1}, and the rate unit is in μmol min^{-1} cm^{-2}.

3.3. Common Electrolyte

The commonly used types of electrolytes currently include $KHCO_3$, $NaHCO_3$, Na_2CO_3, NaOH, etc. Among them, $KHCO_3$ is the most commonly used. Generally, the yield of H_2O_2 by the electrocatalyst is higher in $KHCO_3$ solution, while it is lower in KOH solution. Table 1 summarizes the performance of several representative catalysts reported recently under various conditions.

Table 1. Performance summary of different electrocatalysts for H_2O_2 generation via $2e^-$ WOR.

Catalyst	**Electrolyte**	**^{a}Potential**	H_2O_2 **generation rate**	**FE /%**	**Over -potential/mV**	**Ref**
$ZnGa_2O_4$	2 M K_2CO_3	2.9 V *vs*. RHE	69 μmol cm^{-2} min^{-1}	77	540	[5]
$BiVO_4$	1 M $NaHCO_3$	~ 3.5 V *vs*. RHE	5.77 μmol cm^{-2} min^{-1}	70	—	[6]
WO_3	1 M $NaHCO_3$	~ 2.7 V *vs*. RHE	0.57 μmol cm^{-2} min^{-1}	48	—	[6]
TiO_2	1 M $NaHCO_3$	~ 3.7 V *vs*. RHE	1.01 μmol cm^{-2} min^{-1}	19	—	[6]
SnO_2	1 M $NaHCO_3$	~ 3.3 V *vs*. RHE	1.53 μmol cm^{-2} min^{-1}	50	—	[6]
$CaSnO_3$ (850 °C)	2 M $KHCO_3$	2.6 V *vs*. RHE	347.7 μmol min^{-1} g^{-1}	—	—	[7]
$CaSnO_3$@CF	2 M $KHCO_3$	2.85 V *vs*. RHE	38 μmol cm^{-2} min^{-1}	90	150	[8, 9]
Mo/Bi_2WO_6	2 M $KHCO_3$	3.4 V *vs*. RHE	5.0 μmol cm^{-2} min^{-1}	79	640	[10]
PTFe$^-$GC	1 M Na_2CO_3	2.4 V *vs*. RHE	23.4 μmol cm^{-2} min^{-1}	66	—	[11]
ZnO (1010)	2 M $KHCO_3$	2.6 V *vs*. RHE	4.15 μmol cm^{-2} min^{-1}	81	40	[12]
$BiVO_4$	2 M $KHCO_3$	3.3 V *vs*. RHE	5.5 μmol cm^{-2} min^{-1}	95	—	[13]
Gd/$BiVO_4$	2 M $KHCO_3$	2.6 V *vs*. RHE	2.5 μmol cm^{-2} min^{-1}	78	110	[14]
$CaSnO_3$	2 M $KHCO_3$	3.4 V *vs*. RHE	4.4 μmol cm^{-2} min^{-1}	76	230	[15]
Sb_2O_3	2 M $KHCO_3$	3.08 V *vs*. RHE	0.26 μmol cm^{-2} min^{-1}	22	—	[16]
$CuWO_4$:Sn	2 M $KHCO_3$	2.5 V *vs*. RHE	11.6 μmol cm^{-2} min^{-1}	72	740	[17]
BDD	2 M $KHCO_3$	3.17 V *vs*. RHE	19.7 μmol cm^{-2} min^{-1}	28	—	[18]
C, N doped TiO_2 (600 N)	0.05 M Na_2SO_4	2.66 V *vs*. Ag/AgCl	0.29 μmol L^{-1} cm^{-2} h^{-1}	13	C, N doped TiO_2 (600 N)	[19]
BDD	2 M K_2CO_3/$KHCO_3$ (salt ratios 1:1)	2.85 V *vs*. RHE	76.4 μmol cm^{-2} min^{-1}	87	1190	[2]

4. Types of Catalysts and Modification Methods

4.1. Types of Catalysts that Produce H_2O_2

The commonly used catalysts for producing H_2O_2 currently include two types: carbon-based materials and metal oxides.

Carbon-based materials. For instance, according to Pangotra's report, commercial carbon materials can be utilized to generate electrocatalytic water oxidation of H_2O_2. Such materials include Carbon fiber paper (CFP), carbon cloth (CC), carbon gas diffusion layer (C-GDL), carbon felt (CF), and Glassy carbon (GC). Their respective H_2O_2 production rates in a 2 M $KHCO_3$ electrolyte can reach 190.9, 117.2, 87.3, 83.5, and 82.0 μmol L^{-1}. According to Wang's report, the H_2O_2 production rates of amorphous graphite, normal graphite, and oxidized carboxylated graphite in a 2 M $KHCO_3$ electrolyte were 3.05, 17.47, and 79.2 μM min^{-1} cm^{-2}, respectively. According to Sun's report, the H_2O_2 production of intrinsic carbon defect-rich carbon nanofibers in a 1 M Na_2CO_3 electrolyte (with a pH of 11.83) can reach 22.6 mmol min^{-1} cm^{-2}. Additionally, some other carbon materials can also be used for electrocatalytic production of H_2O_2.

Metal oxides. Unlike the oxygen reduction reaction, the study of water oxidation focuses on the oxygen release activity at the oxidation surface. Among the reported catalysts, RuO_2 and IrO_2 have the highest catalytic activity. It has been determined that their scarcity and high cost limit their large-scale application. Additionally, from the perspective of energy storage, water oxidation forms H_2O_2/H_2 might be another more valuable option compared to O_2/H_2, and it has the ideal advantage of generating a more useful oxidant than O_2. However, these catalysts are unstable when operating at high potentials. Mac Farlane and his colleagues were the first to report that MnOx electrocatalyst can effectively catalyze the WOR to generate H_2O_2 with a lower overpotential. The yield of H_2O_2 was determined to be 77% through the potassium permanganate oxidation experiment. The author attributes the efficiency loss of MnOx to the competitive process between the four-electron pathway to O_2, the chemical disproportionation of H_2O_2, and its further oxidation to water, especially in alkaline media and in the presence of ammonia. Recently, Nørskov and his colleagues have developed a new type of dispersion device, which can directly utilize sunlight to split water into H_2O_2 and H_2 simultaneously. The generated H_2O_2 can be directly used to oxidize the organic substances in water, while hydrogen gas bubbles out and escapes. To make this device possible, an electrocatalyst is needed that can oxidize water to produce H_2O_2, while inhibiting the thermodynamic pathway that is conducive to the generation of O_2 with four electrons. By using thermodynamic analysis based on DFT calculations, they demonstrated that the free energy of the adsorbed OH* can be used to determine the trend of the two-electron oxidation of H_2O to form H_2O_2. Based on this, they discovered that SnO_2 and TiO_2 are excellent candidate materials for generating H_2O_2. This work provides a quantitative basis for identifying effective and selective electrocatalyst materials. Furthermore, WO_3, $BiVO_4$, MnO_2 and SnO_2 are located in the green area and can also effectively produce H_2O_2.

4.2. Catalyst Modification Methods

4.2.1. Morphology and Structural Regulation

Compared with the original materials, nano-materials with different morphologies have different specific surface areas and reaction active sites, which leads to different catalytic performances. Therefore, the catalytic performance of anodes can be improved by controlling morphology. By controlling morphology to enhance the catalytic performance, the morphologies that have been reported in current researches include nanosheets, nanorods and nanoblocks, etc. Here, Zhang [9] pointed out a conductive carbon fiber membrane with abundant oxygen vacancies (Ov), which is fixed by a nanostructured perovskite (a new type of material with $2e^-$ catalysts) (Figure 3). The carbon fiber membrane perovskite ($CaSnO_3$) can be directly used as an independent electrode, and the generation rate of its hydroxide reaches 39.8 μmol per minute, with a selectivity of approximately 90% at 2.9 V vs. RHE. The design of $CaSnO_3$@carbon fiber not only enhances the conductivity and stability of the catalyst but also improves the underlying activity of the perovskite. The density calculation based on functional theory further indicates that oxygen vacancies increase the adsorption of free energy of the oxygen intermediates related to the four-electron hydrogenation pathway, thereby enhancing the oxidation activity and selectivity of $2e^-$ WOR.

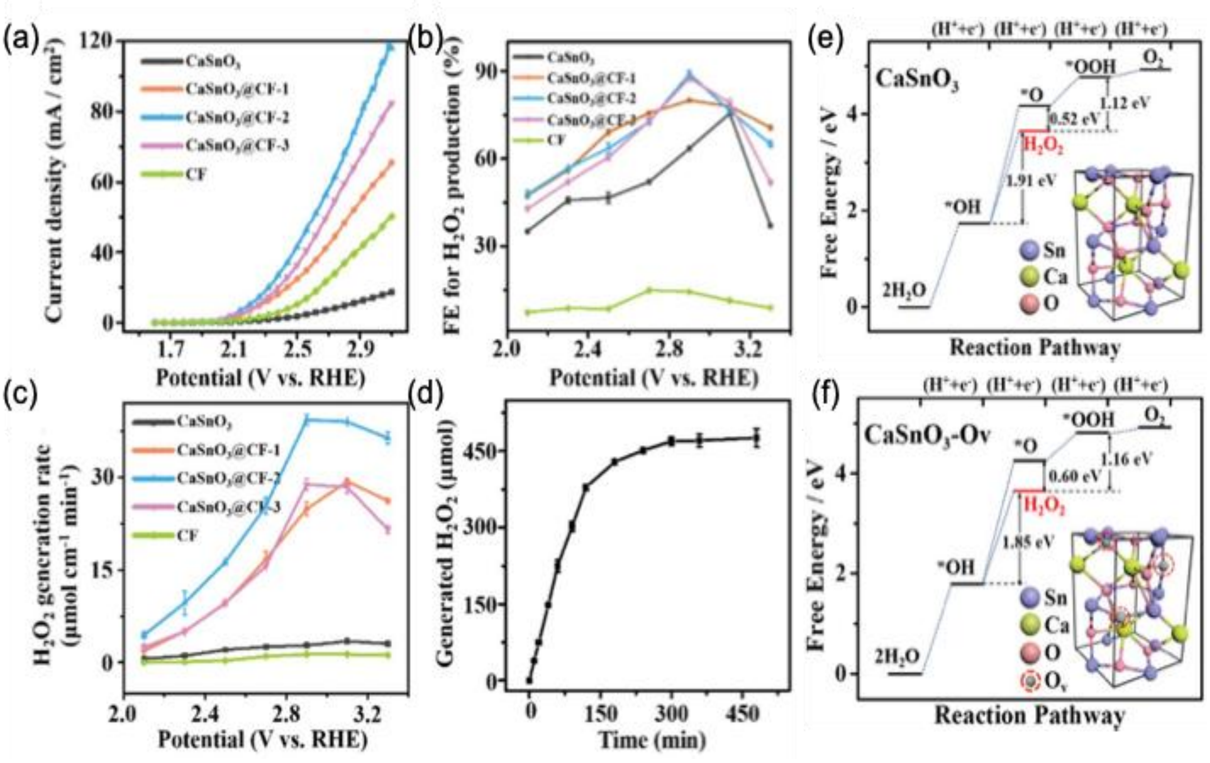

Figure 3. Morphology and structural regulation for $CaSnO_3$.

4.2.2. Facet Regulation

Cleaved surface engineering is regarded as an emerging strategy for adjusting physical and chemical properties and optimizing the photoactivity of materials. It is worth noting that different crystal faces possess anisotropic surface electronic structures, redox reaction sites, surface built-in electric fields, and reactive activities. Therefore, by controlling the crystal planes, the surface electronic structure and built-in electric field can be indirectly modified, thereby affecting the charge migration and leading to an increase in the catalytic activity of catalysts. Crystal facet regulation is an effective method for enhancing the performance of electrocatalytic H_2O_2 generation. This method can selectively expose crystal facets that are conducive to H_2O_2 production, thereby improving the selectivity (FE) of H_2O_2. Nørskov group [12] demonstrated that the $(10\bar{1}0)$ crystal plane of ZnO has significant superiority in water oxidation to produce H_2O_2, far exceeding that of (0001) ZnO, through DFT calculations and experimental data. At a current density of 0.1 mA cm^{-2}, the overpotential of $(10\bar{1}0)$ ZnO is only 40 mV, while FE can reach 81%. The SEM images of $(10\bar{1}0)$ and (0001) ZnO are shown in Figure 4. The (0001) ZnO appears as ordinary granular particles, while $(10\bar{1}0)$ ZnO exhibits regular nanocolumnar structures. Furthermore, the current-voltage curve and the FE of H_2O_2 generation indicate that within the entire voltage range of 1.8-3.1 V vs. RHE, $(10\bar{1}0)$ ZnO produced higher current density and FE (81%) compared to (0001) ZnO. Furthermore, through the comparison of the catalysts reported previously, it was found that the FE of $(10\bar{1}0)$ ZnO in generating H_2O_2 was higher than that of $BiVO_4$, SnO_2, TiO_2, WO_3, Al2O3, V2O5, La_2O_3, Bi2O3 and CoO, etc. These catalysts demonstrated their high efficiency in the water oxidation process to produce H_2O_2.

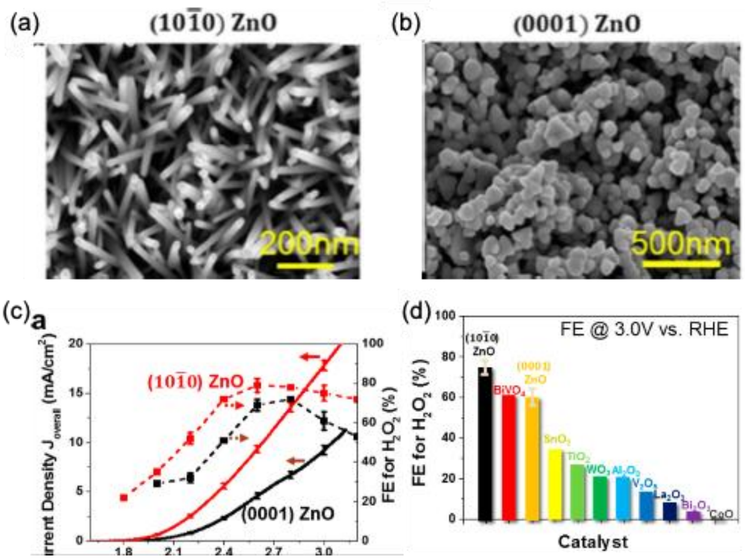

Figure 4. Facet regulation for ZnO.

4.2.3. Doping Method

Simply improving performance by altering one's own appearance is limited. At this point, the strategy of enhancing performance by introducing external elements gradually appears. The method of introducing other elements into semiconductors is called doping. Usually, it aims to change the geometry and electronic structure and regulate the charge carrier density in the original substrate, expanding the charge transfer, thereby increasing the conductivity of the material. In Zhang's research [20], it was found that zinc oxide is an ideal catalyst for $2e^-$ WOR in the field of fuel cells, with good overpotential and stability performance. Subsequently, the electrode was optimized by introducing iron doping (Figure 5). This provides a novel strategy for the on-site advanced oxidation process of generating H_2O_2 based on electrochemical water oxidation. The ZnO and Fe$^-$doped ZnO/Fe prepared by the hydrothermal method are shown in Figure 5a, b. According to Figure 5c and 5d, ZnO/Fe demonstrates superior current signals and H_2O_2 production compared to ZnO. This doping method can also provide a reference for more efficient WOR reactions.

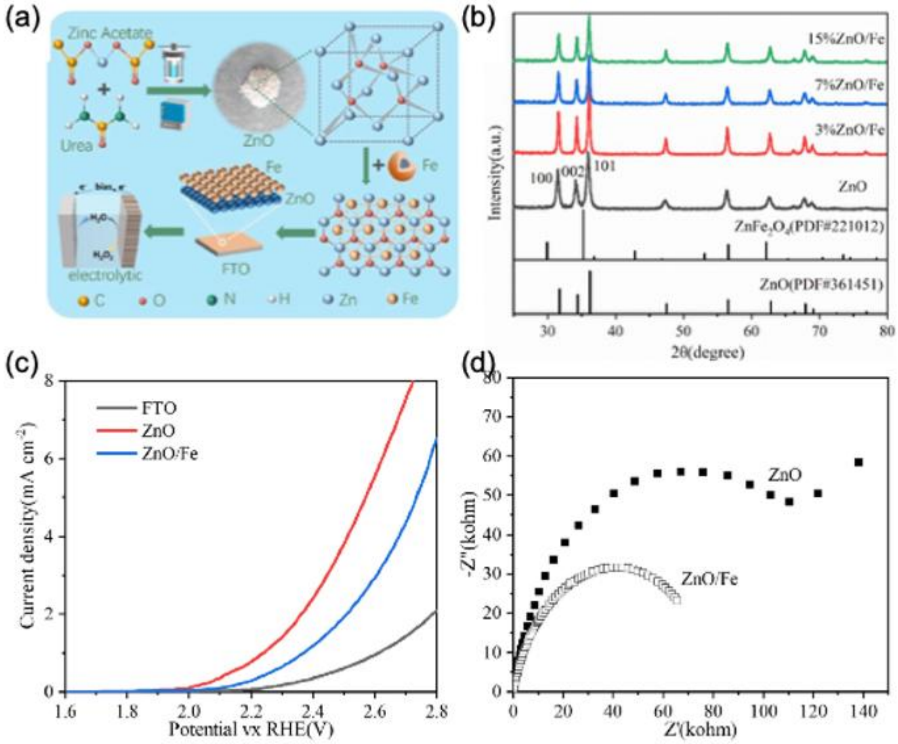

Figure 5. Doping regulation for FTO/ZnO.

4.2.4. Defect Introduction

Introducing defects (such as vacancies, dislocations, doping, etc.) in electrocatalysis can significantly enhance the material performance. Its main advantages include regulating the electronic structure and enhancing the electrical conductivity; creating a large number of unsaturated coordination sites as high-activity centers, optimizing the adsorption energy of reaction intermediates, and reducing the reaction energy barrier; at the same time, defects can increase the specific surface area, promote charge/mass transport, thereby enhancing the catalytic activity and stability. By embedding oxygen-rich zinc oxide nanoparticles into three-dimensional conductive carbon fabric (CC), Zhang [21] successfully prepared a metal oxide/carbon composite electrocatalyst with high selectivity and high H_2O_2 production rate (Figure 6). The effects of different calcination temperatures on the composition and crystallinity of the catalyst were also evaluated. Meanwhile, the relationship between the content of oxygen vacancies and catalytic activity was investigated. The synthesized ZnO/CC-450, as an independent electrode, exhibits outstanding $2e^-$ WOR properties, achieving high selectivity (reaching 72.34% at 2.8 V vs. RHE), high H_2O_2 production rate (17.32 μmol cm^{-2} min^{-1}), and good stability. This sustainable electrochemical two-electron water oxidation process, generated in situ by a simple method and at an economical cost, opens up new avenues for green chemistry.

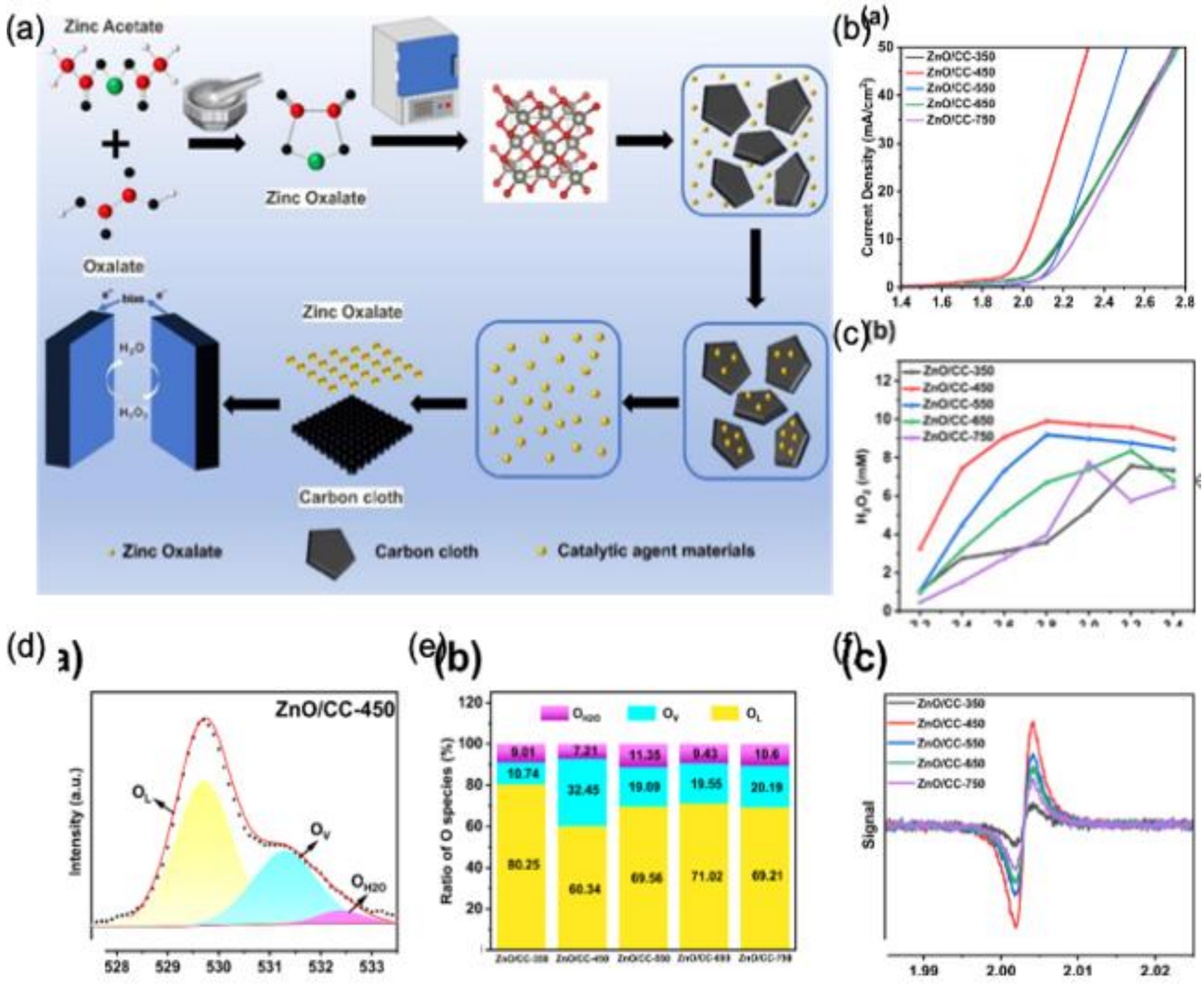

Figure 6. Defect introduction for ZnO/CC.

4.2.5. Interface Engineering

Interface engineering precisely regulates the atomic and electronic structures at the heterogeneous interface of the catalyst, thereby constructing an intrinsically built electric field. This electric field can significantly accelerate the directional migration and separation efficiency of interface charges, effectively reducing the reaction energy barrier. Additionally, the unique interface microenvironment can optimize the adsorption/desorption behaviors of reaction intermediates, simultaneously enhancing the intrinsic activity and stability. It is one of the key strategies for breaking the performance bottleneck of a single component and designing efficient and stable catalysts. In Zhang's report [22], the efficient co-catalyst CO_3O_4 nanoparticles (~10 nm) was deposited on the interface of TiO_2 nanorods/electrolyte to promote the selectivity of oxidative H_2O_2 production. As shown in Figure 7, the positive effect of CO_3O_4 nanoparticles in the $2e^-$ WOR process is to speed up the activation reaction of H_2O to •HO, thus enhancing the H_2O_2 formation. The CO_3O_4/TiO_2 electrode was prepared using a facile dip coating method. The lattice distance (0.479 nm) corresponding to the (111) facet of CO_3O_4 could be found, which showed the close attachment of CO_3O_4 particles on TiO_2 nanorods. The H_2O_2 generation rates and FE values of CO_3O_4/TiO_2 samples with different loading weight were tested to prove the influence of CO_3O_4 nanoparticles on $2e^-$ WOR for H_2O_2. As a result, 0.25 wt% CO_3O_4/TiO_2 anode displayed the highest FE of 26.76% in 0.5 M $KHCO_3$ at 1.23 V vs. RHE, higher than pristine. This works gives an excellent choice to modify electrocatalysts for H_2O_2 generation via $2e^-$ WOR pathway.

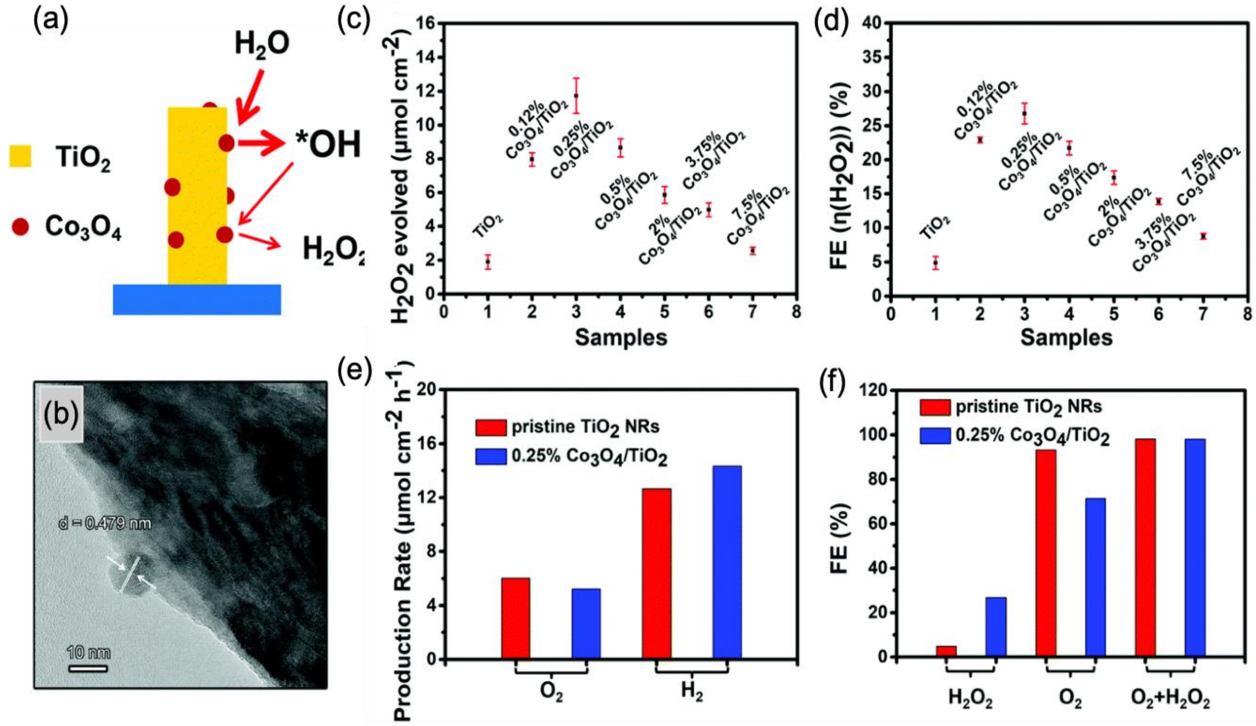

Figure 7. Interface engineering for TiO_2.

4.2.6. Dual Active Site Strategy

The dual active-site strategy overcomes the limitations of a single active site by meticulously constructing two synergistic active centers. These two sites can specifically adsorb and activate different reaction intermediates, achieving functional complementarity and effectively optimizing the energy barriers of multi-step reactions. This not only accelerates the reaction kinetics but also precisely regulates the reaction pathway, significantly enhancing the activity of the catalyst and the selectivity of the target product. It is one of the key strategies for designing efficient electrocatalysts. Li [5] used $ZnGa_2O_4$ with dual active sites as the anode material to enhance selectivity and prevent the decomposition of H_2O_2 (Figure 8). Under the condition of 2.3 V vs. RHE, the FE reached 82% when H_2O_2 was generated through direct (via OH^-) and indirect (via HCO_3^-) pathways. The percarbonate is the key substance generated by converting bicarbonate at the Ga-Ga dual sites. The peroxide bond is stable on the $ZnGa_2O_4$ anode surface, significantly improving the selectivity.

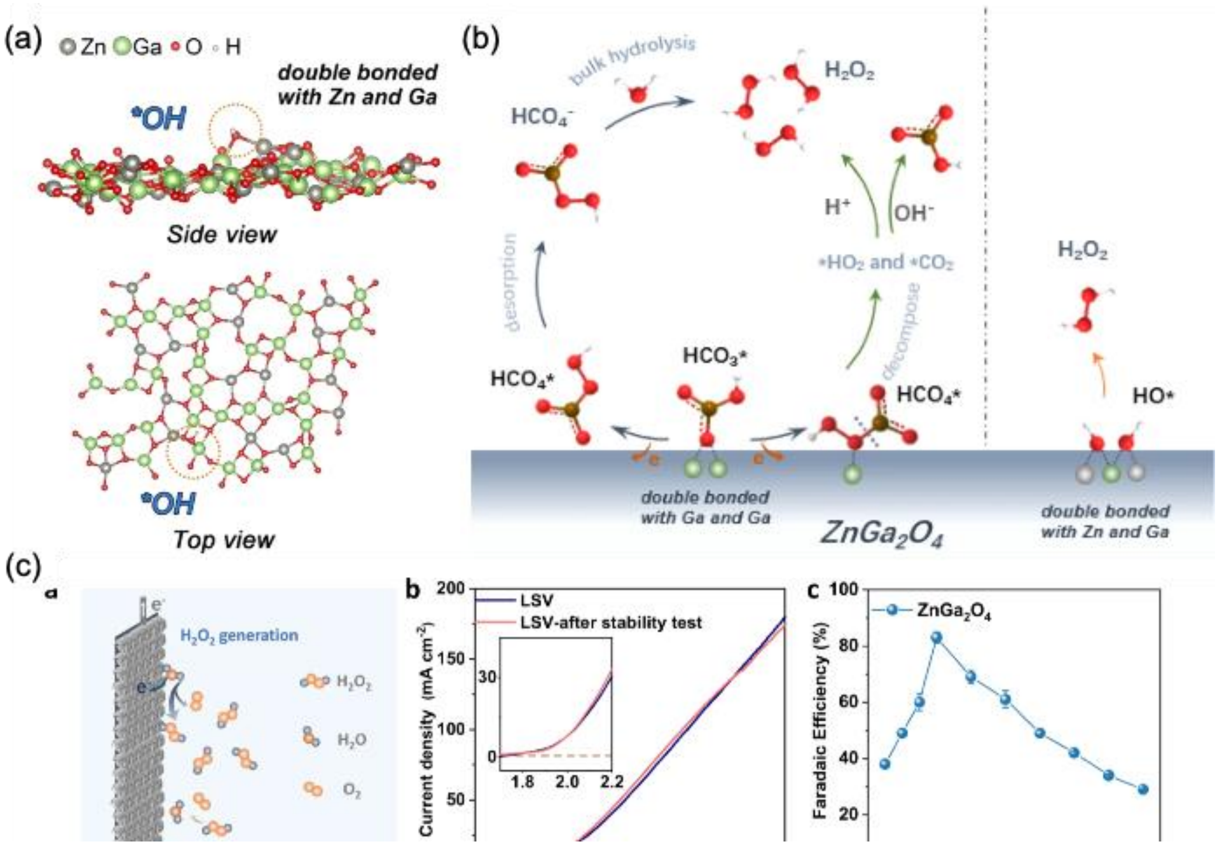

Figure 8. Dual active site strategy for $ZnGa_2O_4$.

4.2.7. Series Connection of Anode and Cathode

This strategy innovatively couples the anodic oxidation reaction with the cathodic reduction reaction within the same system, using the products of the anodic reaction as the reactants for the cathodic reaction. Its core value lies in: replacing or assisting the high-energy-consuming cathodic hydrogen evolution reaction, simultaneously producing high-value chemicals, significantly improving atomic and economic efficiency; at the same time, reducing the overall cell voltage and achieving a substantial decrease in system energy consumption. This strategy provides a new paradigm for collaborative synthesis and energy conversion under green electricity drive. Wang [23] designed and fabricated a single-atom doped with nickel titanium dioxide electrocatalyst (Figure 9), which was used to generate H_2O_2 through 2e$^-$ WORs at the cathode, with a FE of up to 90%. This catalyst was also combined with the ORR at the cathode, and in a full cell device, H_2O_2 was simultaneously produced at a high current. This full cell device exhibited excellent stability and achieved a 146% FE at 240 mA cm^{-2}, providing a potential solution for on-site H_2O_2 generation.

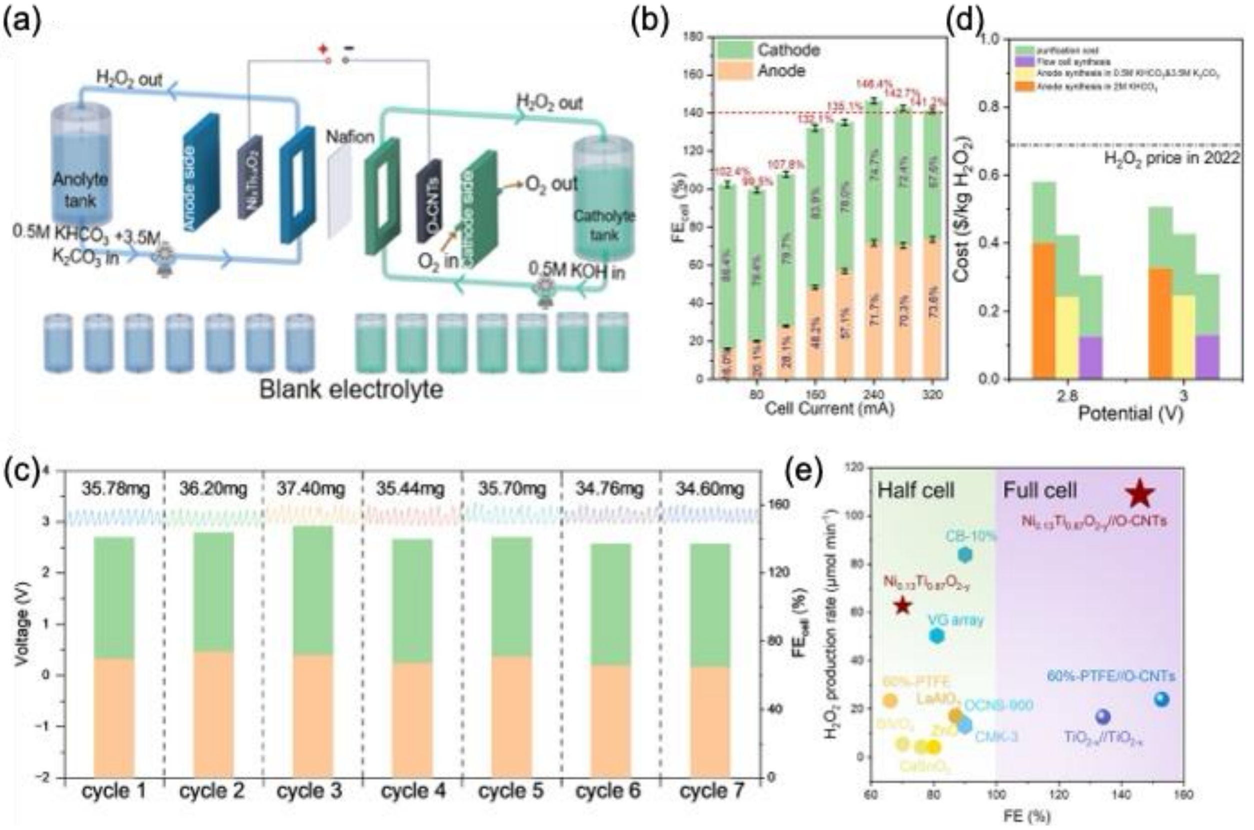

Figure 9. Strategy of Series connection of anode and cathode.

5. Environmental Applications

As an efficient and environmentally friendly oxidant, H_2O_2 has demonstrated great potential in the field of environmental applications. Although there have been reports on the production of H_2O_2 through $2e^-$ WOR, its application in the field of environmental protection is still relatively rare. Up to now, the in-situ electrochemical H_2O_2 generation applications achieved through $2e^-$ WOR have mainly been applied in disinfection and pollutant degradation. Generally speaking, during the reaction process, some reactions related to oxygen will occur, and these reactions will also play a role in the formation of H_2O_2.

$$O_2 + e^- \rightarrow O_2^{\bullet -} \quad E^0 = -0.33 \text{ V vs. RHE} \tag{5}$$

$$O_2^{\bullet -} + H^+ \rightarrow HOO\bullet \tag{6}$$

$$O_2^{\bullet -} + HOO\bullet \rightarrow HOO- + O_2 \tag{7}$$

$$HOO\bullet + e^- \rightarrow HOO^- \quad E^0 = -0.74 \text{ V vs. RHE} \tag{8}$$

Related to this, H_2O_2 can undergo reduction reactions or endogenous reactions, thereby forming •OH with strong oxidizing properties.

$$H_2O_2 + e^- \rightarrow \bullet OH + OH^- \quad E^0 = 0.10 \text{ V } \textit{vs}\text{. RHE} \tag{9}$$

$$H_2O_2 \rightarrow 2\bullet OH \tag{10}$$

$$O^{\bullet} + H+ + e^- \rightarrow H_2O \qquad E^0 = 2.73 \text{ V } \textit{vs}\text{. RHE} \tag{11}$$

During the reaction process, some oxygen-containing substances such as $O_2^{\bullet -}$ and •OH usually have strong oxidation capacity and can be used for pollution control and environmental remediation. In particular, $2e^-$ WOR can be used in water bodies contaminated by bacteria, deep soil, plateaus, and many other anoxic or oxygen-free environments because it does not rely on oxygen supply. This is the unique advantage of the $2e^-$ WOR process over the $2e^-$ ORR process. The simulation disinfection test in Li's work [24] fully demonstrated this advantage by comparing the water purification performance of $2e^-$ WOR and $2e^-$ ORR in a reactor containing N2 gas (anoxic conditions). Within 45 minutes, the CC/$CuWO_4$ anode killed 100% of the bacteria, while the disinfection efficiency of the CP/CNT cathode was only slightly less than 4%. Moreover, the in-situ MB degradation efficiency of the CC/$CuWO_4$ anode and the CP/CNT cathode is similar to their disinfection performance. These results fully demonstrate the advantages of $2e^-$ WOR in the generation of H_2O_2 for disinfection and pollutant degradation.

5.1. Degradation of Organic Pollutants

In recent years, research on the effective degradation of organic pollutants in soil and water environments using ROS (H_2O_2, $O_2^{\bullet -}$, •OH) has gradually unfolded. H_2O_2 helps degrade pollutants such as dyes, antibiotics, phenols and drugs. Organic pollutants can gradually degraded through reactions such as hydrogen atom transfer, electron transfer, and electrophilic addition. For instance, in Li's report [25], the on-site generated H_2O_2 demonstrated outstanding performance in degrading persistent pollutants such as norfloxacin (NFX) and dyes like methylene blue (MB). Both NFX and MB were completely degraded within 140 minutes (Figure 10), and the final total organic carbon (TOC) removal rate reached approximately 88% after 4 hours. And in the on-site H_2O_2 artificial synthesis system, the degradation pathway of NFX. Two main pathways were discovered: quinolone group transformation and piperazine ring cleavage. Path I mainly includes hemolysis and addition reactions, followed by decarboxylation, decarbonylation and hydroxylation reactions. In Path II, the piperazine ring is attacked at the tertiary amine position, thereby triggering a ring opening reaction and subsequently forming an intermediate (with a mass spectrometry value of 294). Subsequently, an intermediate (with a mass spectrometry value of 251) is generated through further oxidation, and a product with a mass spectrometry value of 233 is produced through a defluorination reaction. This work demonstrates the optimization of structural engineering for the formation of H_2O_2 at the anode.

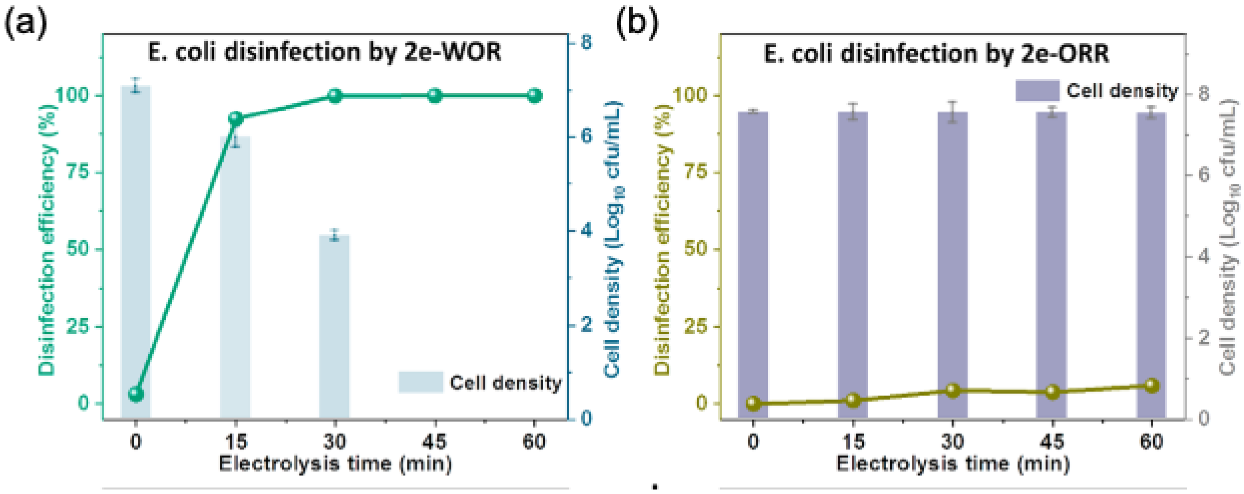

Figure 10. The application of produced H_2O_2 via WOR in pollutant degradation.

5.2. WOR Produces H_2O_2 for Disinfection

H_2O_2 can successfully inactivate bacteria and prevent the generation of disinfection by-products, which is safer and more convenient than the commonly used chlorine disinfection method. It is generally believed that pathogen exposure to reactive oxygen species (ROS) and reactive nitrogen species (RNS) can lead to genomic and protein damage. The fundamental principle of electrochemical disinfection is to use active oxygen (such as H_2O_2, superoxide anion, hydroxyl radicals) to attack pathogens, and then destroy their physiological structure, antioxidant enzymes, respiratory, metabolic systems and other systems. Figure 11 shows the disinfection process of reactive oxygen species [26]. Reactive oxygen species can inactivate infectious pathogens and convert them into organic matter or dead microbial cells, which are then oxidized into water and carbon dioxide [27]. Among them, H_2O_2 plays an irreplaceable role due to its unique molecular form and long lifespan in water. Usually, only a few micromoles of H_2O_2 concentration can effectively inactivate pathogens.

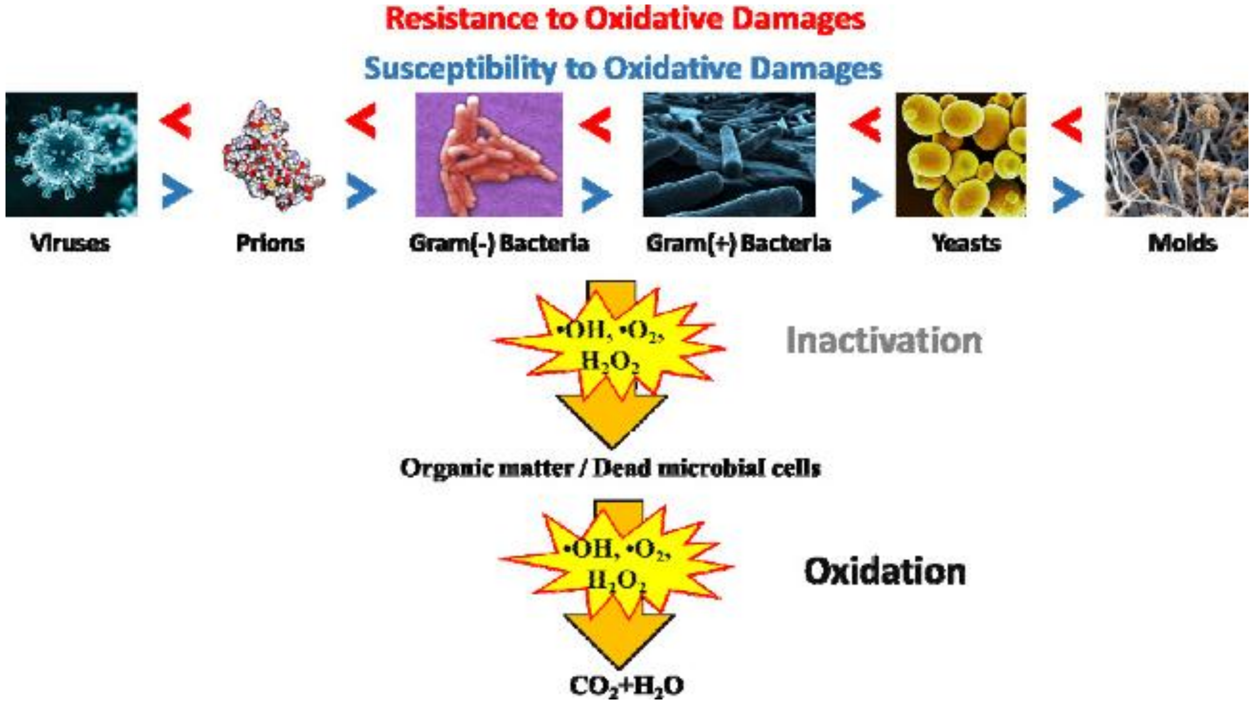

Figure 11. The application of produced H_2O_2 via WOR in disinfection.

Some researchers applied the H_2O_2 produced by WOR to the disinfection treatment of microorganisms in environmental media. The relevant situation is shown in Table 2. For instance, in Li's report, the disinfection capability of the $CuWO_4$ anode was investigated by mixing the generated H_2O_2 with the Escherichia coli suspension. Escherichia coli-K12 (E. coli-K12) was used as the target bacterium. The results show that at a current of 80 mA, the bacterial inactivation rate of the generated H_2O_2 reached 99.5% within 30 minutes, and the cell density of Escherichia coli decreased to approximately 5 log10 cfu mL^{-1}. Furthermore, when the accumulation time of H_2O_2 is extended to 60 min, the disinfection efficiency can reach 100%. Furthermore, under an oxygen-deficient condition, the in-situ water purification carried out by the CC/$CuWO_4$ electrode demonstrated that the bacterial inactivation efficiency reached 99.9% within 30 minutes, and the cell density decreased to approximately 4 log10 cfu mL^{-1}. When the accumulation time of H_2O_2 reached 45 minutes, 100% of the bacteria died. Therefore, these results indicate that the H_2O_2 produced by 2e$^-$ WOR has excellent application potential in water disinfection.

Table 2. The disinfection treatment of H_2O_2 produced by WOR.

Catalyst	Bacterium	Disinfection efficiency	Ref
CC/$CuWO_4$	*E. coli*	~99.5%, 30 min	[24]
SnO_{2-x} /TiO_2	*E. coli, S. aureus, Bacillus subtilis, Listeria innocua, Candida albicans and Bacteriophage MS2*	>99.9999%, ~16 s of retention time	[26]
HPL-coated RuO_2-IrO_2	*E. coli*	>99.9%, 60 min	[28]
Fe$^-$doped ZnO	*E. coli*	99%, 120 min	[20]

6. Conclusion and Prospect

In this review, we summarize the fundamental aspects of H_2O_2 synthesis in the $2e^-$ WOR pathway, including thermodynamics, basic evaluation parameters, DFT calculations regarding surface-dependent selectivity and activity, as well as the influence of electrolytes on $2e^-$ WOR. Then, this paper summarizes various electrocatalysts and their modification strategies to enhance the performance of WOR in producing H_2O_2, including morphology and structure, crystal plane control, doping, defects, interface, dual active site strategy, and anode-cathode series strategy, etc. Subsequently, we reviewed the practical applications of producing H_2O_2 through the $2e^-$ WOR process in the environmental field, including disinfection and pollutant degradation. However, despite many significant accomplishments in the past few years, there are still a large number of interesting issues that require in-depth expansion and expansion in the application of H_2O_2 production in $2e^-$ WOR process.

1) Types of catalysts. At present, the majority of the electrocatalysts used are metal oxides, carbon-based materials, and a small amount of organic compounds. In addition, there are also a wider range of material types such as sulfides, nitrides, their mixtures, and other materials. More types and quantities of stable, resource-rich and low-cost electrocatalysts are still needed.

2) Conduct in-depth research on theoretical calculations, including optimizing the reaction pathway of WOR to produce H_2O_2, and refining the calculations of intermediate adsorption energy and energy barriers, studying the influence of catalyst surface structures (such as defects and doping) on the reaction selectivity. Taking into account the solvent effect and potential influence, simulate the actual reaction environment. Compare different catalyst systems and select materials with high activity and high selectivity.

3) Expand environmental applications. For instance, simulate the reaction pathway of H_2O_2 in degrading pollutants in water bodies/soils, and calculate the reaction energy barrier between it and the pollutants. Study the stability of the catalyst under complex conditions (such as pH and impurity ions) and its influence on the production of H_2O_2 by WOR. Combining DFT screening to efficiently produce environmentally friendly catalysts that can produce H_2O_2, and reducing application costs, etc.

References

[1] Q.J.J. Baek, N.S. Johnson, Y. Jiang, R. Ning, A. Mehta, S. Siahrostami, X. Zheng, Discovery of $LaAlO_3$ as an efficient catalyst for two-electron water electrolysis towards hydrogen peroxide, Nature communications 3 (2022) 7256.

[2] S. Mavrikis, M. Göltz, S.C. Perry, F. Bogdan, P.K. Leung, S. Rosiwal, L. Wang, C. Ponce de León, Effective Hydrogen Peroxide Production from Electrochemical Water Oxidation, ACS Energy Letters 6 (2021) 2369-2377.

[3] S.C. Perry, D. Pangotra, L. Vieira, L.-I. Csepei, V. Sieber, L. Wang, C. Ponce de León, F.C. Walsh, Electrochemical synthesis of hydrogen peroxide from water and oxygen, Nature Reviews Chemistry 3 (2019) 442-458.

[4] X. Hu, Z. Sun, G. Mei, X. Zhao, B.Y. Xia, B. You, Engineering Nonprecious Metal Oxides Electrocatalysts for Two-Electron Water Oxidation to H_2O_2, Advanced Energy Materials 12 (2022) 2201466.

[5] L. Li, Z. Hu, Y. Kang, S. Cao, L. Xu, L. Yu, L. Zhang, J.C. Yu, Electrochemical generation of hydrogen peroxide from a zinc gallium oxide anode with dual active sites, Nature communications 14 (2023) 1890.

[6] X. Shi, S. Siahrostami, G.L. Li, Y. Zhang, P. Chakthranont, F. Studt, T.F. Jaramillo, X. Zheng, J.K. Norskov, Understanding activity trends in electrochemical water oxidation to form hydrogen peroxide, Nature communications 8 (2017) 701.

[7] T. Kang, B. Li, Q. Hao, W. Gao, F. Bin, K.N. Hui, D. Fu, B. Dou, Efficient Hydrogen Peroxide (H_2O_2) Synthesis by $CaSnO_3$ via Two-Electron Water Oxidation Reaction, ACS Sustainable Chemistry & Engineering 8 (2020) 15005-15012.

[8] J. Wu, H. Zhou, Q. Li, M. Chen, J. Wan, N. Zhang, L. Xiong, S. Li, B.Y. Xia, G. Feng, M. Liu, L. Huang, Densely Populated Isolated Single Co-N Site for Efficient Oxygen Electrocatalysis, Advanced Energy Materials 9 (2019) 1900149.

[9] C. Zhang, R. Lu, C. Liu, L. Yuan, J. Wang, Y. Zhao, C. Yu, High Yield Electrosynthesis of Hydrogen Peroxide from Water Using Electrospun $CaSnO_3$@Carbon Fiber Membrane Catalysts with Abundant Oxygen Vacancy, Advanced Functional Materials 31 (2021) 2100099.

[10] J. Zhang, G. Zhang, Q. Ji, H. Lan, J. Qu, H. Liu, Carbon nanodot-modified FeOCl for photo-assisted Fenton reaction featuring synergistic in-situ H_2O_2 production and activation, Applied Catalysis B: Environmental 266 (2020) 118665.

[11] C. Xia, S. Back, S. Ringe, K. Jiang, F. Chen, X. Sun, S. Siahrostami, K. Chan, H. Wang, Confined local oxygen gas promotes electrochemical water oxidation to hydrogen peroxide, Nature Catalysis 3 (2020) 125-134.

[12] S.R. Kelly, X. Shi, S. Back, L. Vallez, S.Y. Park, S. Siahrostami, X. Zheng, J.K. Nørskov, ZnO As an Active and Selective Catalyst for Electrochemical Water Oxidation to Hydrogen Peroxide, ACS Catalysis 9 (2019) 4593-4599.

[13] X. Shi, Y. Zhang, S. Siahrostami, X. Zheng, Light-Driven $BiVO_4$-C Fuel Cell with Simultaneous Production of H_2O_2, Advanced Energy Materials 8 (2018) 1801158.

[14] J.H. Baek, T.M. Gill, H. Abroshan, S. Park, X. Shi, J. Nørskov, H.S. Jung, S. Siahrostami, X. Zheng, Selective and Efficient Gd-Doped $BiVO_4$ Photoanode for Two-Electron Water Oxidation to H_2O_2, ACS Energy Letters 4 (2019) 720-728.

[15] S.Y. Park, H. Abroshan, X. Shi, H.S. Jung, S. Siahrostami, X. Zheng, $CaSnO_3$: An Electrocatalyst for Two-Electron Water Oxidation Reaction to Form H_2O_2, ACS Energy Letters 4 (2018) 352-357.

[16] Y. Wang, X. Lian, Y. Zhou, W. Guo, H. He, Synthesis and characterization of Sb2O_3: a stable electrocatalyst for efficient H_2O_2 production and accumulation and effective degradation of dyes, New Journal of Chemistry 45 (2021) 8958-8964.

[17] L. Li, L. Xu, A.W.M. Chan, Z. Hu, Y. Wang, J.C. Yu, Direct Hydrogen Peroxide Synthesis on a Sn-doped $CuWO_4$/Sn Anode and an Air-Breathing Cathode, Chem. Mater. 34 (2021) 63-71.

[18] S. Mavrikis, M. Göltz, S. Rosiwal, L. Wang, C. Ponce de León, Boron-Doped Diamond Electrocatalyst for Enhanced Anodic H_2O_2 Production, ACS Applied Energy Materials 3 (2020) 3169-3173.

[19] S.-g. Xue, L. Tang, Y.-k. Tang, C.-x. Li, M.-l. Li, J.-j. Zhou, W. Chen, F. Zhu, J. Jiang, Selective Electrocatalytic Water Oxidation to Produce H_2O_2 Using a C,N Codoped TiO_2 Electrode in an Acidic Electrolyte, ACS applied materials & interfaces 12 (2019) 4423-4431.

[20] M. Zhang, J. Yan, D. Wang, X. Dong, H. Ma, H. Wei, G. Wang, Anodic water oxidation to H_2O_2 on Fe^{-}doped ZnO for electro-Fenton wastewater purification, Electrochim. Acta 464 (2023) 142940.

[21] Y. Zhang, Z. Lin, D. Zhang, Y. Zheng, M. Huang, C. Jin, J. Zhang, Anodic Water Oxidation to H_2O_2 on Ov-Rich ZnO Nanoparticles for Degradation of Tetracycline, ACS Appl. Nano Mater. 8 (2025) 3356-3367.

[22] J. Zhang, Z. Luo, T. Wang, J. Gong, Highly Efficient Photoelectrochemical H_2O_2 Production Reaction with CO_3O_4 as Co-catalysts, Chem. Commun. 54 (2018) 7026-7029.

[23] Z. Wang, M.G. Sendeku, W. Xu, S. Chen, B. Tian, F. Wang, Y. Kuang, X. Sun, Highly efficient paired H_2O_2 production through 2e^{-} water oxidation coupled with 2e^{-} oxygen reduction, Chem Catalysis 3 (2023) 100672.

[24] L. Li, K. Xiao, P.K. Wong, Z. Hu, J.C. Yu, Hydrogen Peroxide Production from Water Oxidation on a $CuWO_4$ Anode in Oxygen-Deficient Conditions for Water Decontamination, ACS applied materials & interfaces 14 (2022) 7878-7887.

[25] L. Li, J.C. Yu, On-Demand Synthesis of H_2O_2 by Water Oxidation for Sustainable Resource Production and Organic Pollutant Degradation, Angew.Chem. Int. Ed. 59 (2020) 20538–20544.

[26] Y. Zeng, Electrocatalytic H_2O_2 generation for disinfection, Chinese Journal of Catalysis 42 (2021) 2149–2163.

[27] J. Zhang, S. Qu, B. Li, R. Yu, L. Ling, X.-Y. Li, Synergetic physical damage and chemical oxidation for highly efficient and residue^{-}free water disinfection, Nature Water 2 (2024) 1226–1237.

[28] K. Yi, High H_2O_2 production in membrane^{-}free electrolyzer via anodic bubble shielding towards robust rural disinfection, Nature communications 16 (2025) 1893.